Stacking-Faults in Tellurium-Doped Gallium Arsenide

D. LAISTER, G. M. JENKINS
Department of Metallurgy, University College, Swansea, Glam, UK

Received 15 August 1967, and in revised form 10 May 1968

Samples of bulk-grown gallium arsenide single crystals, taken from both static freeze, and Czochralski ingots doped to a high level with tellurium, have been examined using transmission electron microscopy. Observation of single and multiple stacking-fault layers which have fault vectors of the kind $R = \frac{a}{3} < 111 >$ is reported. It is shown by diffraction contrast experiments that the stacking-fault defects are extrinsic. They are thought to be rafts of tellurium substituting for arsenic in $\{111\}$ planes. The prevalence of the observed layer defects correlates well with the increase in carrier concentration in certain regions of the crystals.

1. Introduction

As part of an investigation into the nature of the substructure of gallium arsenide, tellurium-doped specimens of bulk-grown material have been examined using transmission electron microscopy. The nature of the defect population of the bulk-grown crystals characterises substrate material for electrical devices, especially with regard to solid-state lasers and electroluminescent diodes. The efficiency of solid state devices in general is known to decrease rapidly for carrier concentrations (N) > 10^{18}/cm^3. It is shown here that a characteristic feature of such material is a high population of the stacking-faults which are the subject of the present analysis.

In previous microstructural studies Meieran [1] has observed precipitates and stacking-faults in Te-doped GaAs, the precipitates only being observed when $N > 2 \times 10^{18}$/cm^3. Abrahams *et al* [2] have shown that in selenium-doped GaAs the prominent features of the substructure are stacking-faults, twins, and precipitates [3]. Their investigations were made mainly on epitaxial layers prepared by homoepitaxial vapour deposition, and not on bulk crystals.

In this paper it is shown that a common feature of heavily-doped areas of GaAs single crystals prepared by gradient-freeze and Czochralski methods is a high concentration of layer-defects, the nature of which has been determined by contrast techniques.

2. Experimental

Slices of gallium arsenide single crystal were obtained from two sources. The first was a crystal grown by the gradient freeze method, using a stoichiometric atmosphere of arsenic with a known temperature profile and a freezing rate of approximately 2.5 mm/h. The second was a crystal grown by a Czochralski technique employing liquid encapsulation.

The crystal prepared by the gradient freeze method had been doped with Te to give a carrier concentration at its impure end of $N \approx 5 \times 10^{18}$/cm^3, while the Czochralski-grown crystal had a carrier concentration of $N \approx 8 \times 10^{18}$/cm^3 at its impure end. The slices which were oriented (100) for examination were selected from various parts of the crystals from pure to impure ends to study the effects of the growth procedures. These slices were then lapped on 6 μm grade alumina to a thickness of 0.004 $\pm$ 0.001 in. (1.0 in. = 2.5 cm). From these slices, 2.3 mm diameter discs were cut ultrasonically to fit the specimen holder of the high-tilt ($\pm$ 30°) cartridge of the AEI-EM6G electron microscope. The discs were then thinned using a modified Buiocchi technique [4] to render them suitable for examination by electron trans-

mission. This modified thinning technique gives exceptionally close control of the thinning, and large areas are found suitable for electron transmission. Great care must be exercised in the handling of the foils, as they are extremely fragile due to the two $\{110\}$ cleavage planes which intersect the foil plane at right angles.

3. Observations

3.1. General

A general area showing stacking-fault defects is shown in fig. 1. The foil thickness in this region

Figure 1 Transmission electron micrograph of stacking-faults in Te-doped GaAs, $g = 0\,2\,2$; only one set of faults is visible ($\xi_g S_g = 0$).

was about 3500 Å, and the area occupied by the faults approximately 25 μm^2. Smaller areas were also observed in specimens taken from the pure end of the crystal with correspondingly fewer stacking-faults. The GaAs foils were oriented with (100) normal to the incident electron beam, and the layer-defects were seen to lie in orthogonal directions. It will be shown in the following sections that these faults lie on $\{111\}$ planes. With a (100) oriented foil there are four different $\{111\}$ planes inclined at 54.7° to the foil surface, and these intersect the (100) surface along two $< 110 >$ directions perpendicular to each other. The planar defects were of varying size; single-layer defects were of the order of 0.5 μm in size, while two and three-layer loops were 1 μm and 1.5 μm respectively, measured along a $< 110 >$ direction. The second and third layers were not symmetrically placed in relation to the first layer like the stacking-faults associated with quenching experiments in aluminium [5, 6]; nor had they a characteristic regular shape.

Additional features present in these heavily-faulted regions were tangles of dislocations. Such heavily-faulted regions occurred more frequently in the impure end of the crystal, i.e. for $N \approx 10^{18}/cm^3$. For $N \approx 10^{19}/cm^3$ discrete precipitates were seen lying on $\{100\}$ planes as observed by Meieran [1] but these will not be discussed here.

3.2. Nature of the Faults

When the regions of high stacking-fault density were examined using the selected area diffraction method no reflections additional to those of the GaAs parent lattice were detected. It is concluded therefore that the defects are stacking-faults and not micro-twins.

All the faults showed fringe contrast for each of the four 400 reflections; two of these reflections are shown in fig. 2a, b. For 220 reflections the faults lying parallel to the g vector were invisible (see fig. 1). Therefore R is a vector lying in the $\{220\}$ planes plus some arbitrary vector. From observation of the four 220 reflections ($g = 022, 0\bar{2}2, 02\bar{2}, 0\bar{2}\bar{2}$) it follows that

$$R = \kappa < 111 > + R_0$$

R_0 being an arbitrary lattice vector [9]. The value of κ can be obtained from the observation of the defects using the 311 reflections about the [310] and [301] normals; using fig. 5 compare table I with fig. 3a, b, c, d. Therefore, using the argument given by Booker and Tunstall [7] $R = \pm\frac{1}{3} < 111 >$ for a fault. When R is positive the fault is extrinsic, and when R is negative the fault is intrinsic. Gevers *et al* [8] have shown how the nature of the fault, and how the sign of R, can be determined from the dark field image. For 220, 400 reflections, g points away from the light fringe if the fault is intrinsic, and towards it if it is extrinsic. This method was employed using high-resolution

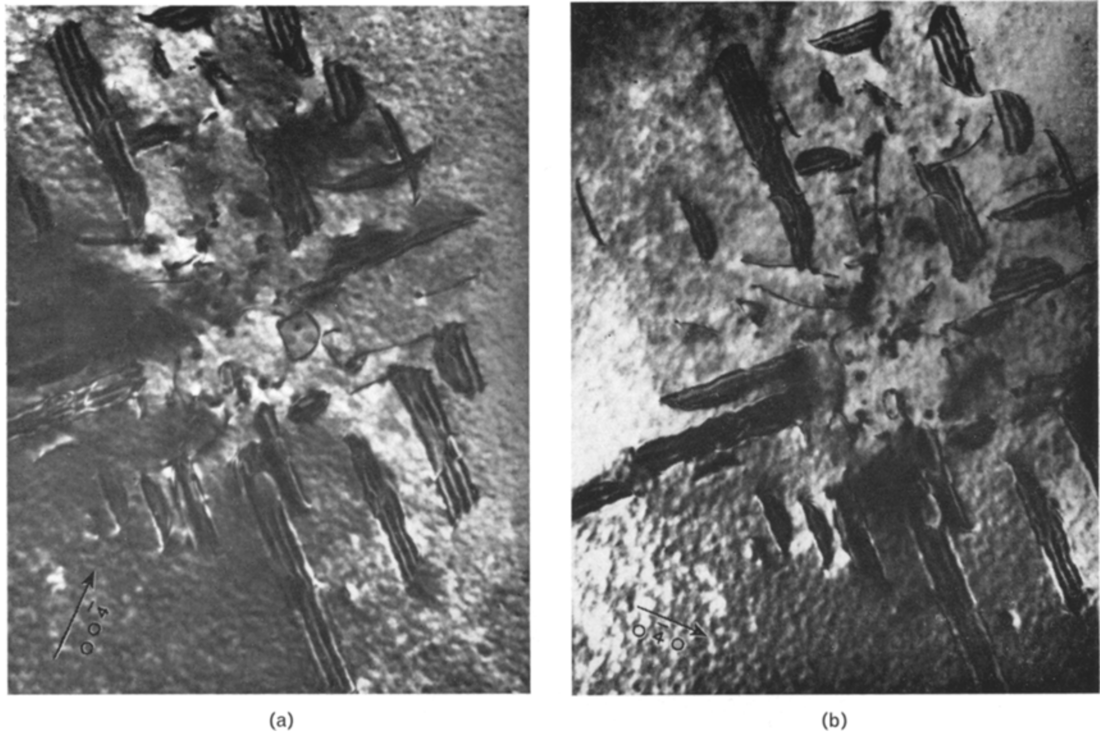

Figure 2 Transmission electron micrograph of stacking-faults showing the contrast obtained using 400 reflections. (a) $g = 00\bar{4}$; (b) $g = 0\bar{4}0$ ($\xi_g S_g = 0$).

TABLE I Value of *g.R* for the reflections used in the fault analysis.

g	R $\frac{1}{3}[111]$	$\frac{1}{3}[\bar{1}11]$	$\frac{1}{3}[\bar{1}\bar{1}1]$	$\frac{1}{3}[1\bar{1}1]$
		$g \cdot R$		
$\bar{1}13$	+1	+5/3	+1	+1/3
11'3	−1/3	−1	−5/3	−1/3
$\bar{1}31$	+1	+5/3	−1	−1/3
$\bar{1}3\bar{1}$	+1/3	+1	−1	−5/3
022	+4/3	+4/3	0	0
$02\bar{2}$	0	0	−4/3	−4/3
$0\bar{2}2$	0	0	+4/3	+4/3
004	+4/3	+4/3	+4/3	+4/3
$0\bar{4}0$	−4/3	−4/3	+4/3	+4/3

dark field, to determine the sign of R for single faults intersecting the top and bottom of the foil for the layer defects reported here. Care was taken to observe only single-layer faults as the multiple-layer faults give rise to anomalous images when examined in high-resolution dark field. The analysis showed the R was positive rather than negative, and hence single faults were extrinsic.

The fringe contrast in the second and third layer of the faults can be explained in terms of the lattice displacement. The faults were planar when examined edge on (within the resolution of the electron microscope) and so they are considered to consist of overlapping faults on adjacent planes. If this is the case, $R = \frac{1}{3}[111]$ for the first layer of the fault on a (111) plane. For the second layer, $R = \frac{2}{3}[111]$ and for the third layer $R = \frac{3}{3}[111]$. Hence the corresponding values of $g \cdot R$ are $+\frac{4}{3}, +\frac{8}{3}, +\frac{12}{3}$, when $g = 022$. The value $\frac{12}{3}$ is an integer, and hence no fringe contrast should be seen in the third layer which is the observed case, see fig. 1, where the fault at A should be noted. The fringes in the second layer should be displaced one fringe spacing with respect to the fringes in the first layer, which is the observed case. The fringe spacings in faults showing fringe contrast vary because of the variation in extinction distance for the operating reflection, this being smallest for a 220 reflection and largest for a 400 reflection. This compares well with values of the extinction distance we have computed for GaAs. The actual value of the fault vector R is not certain but can be resolved if the diffraction contrast

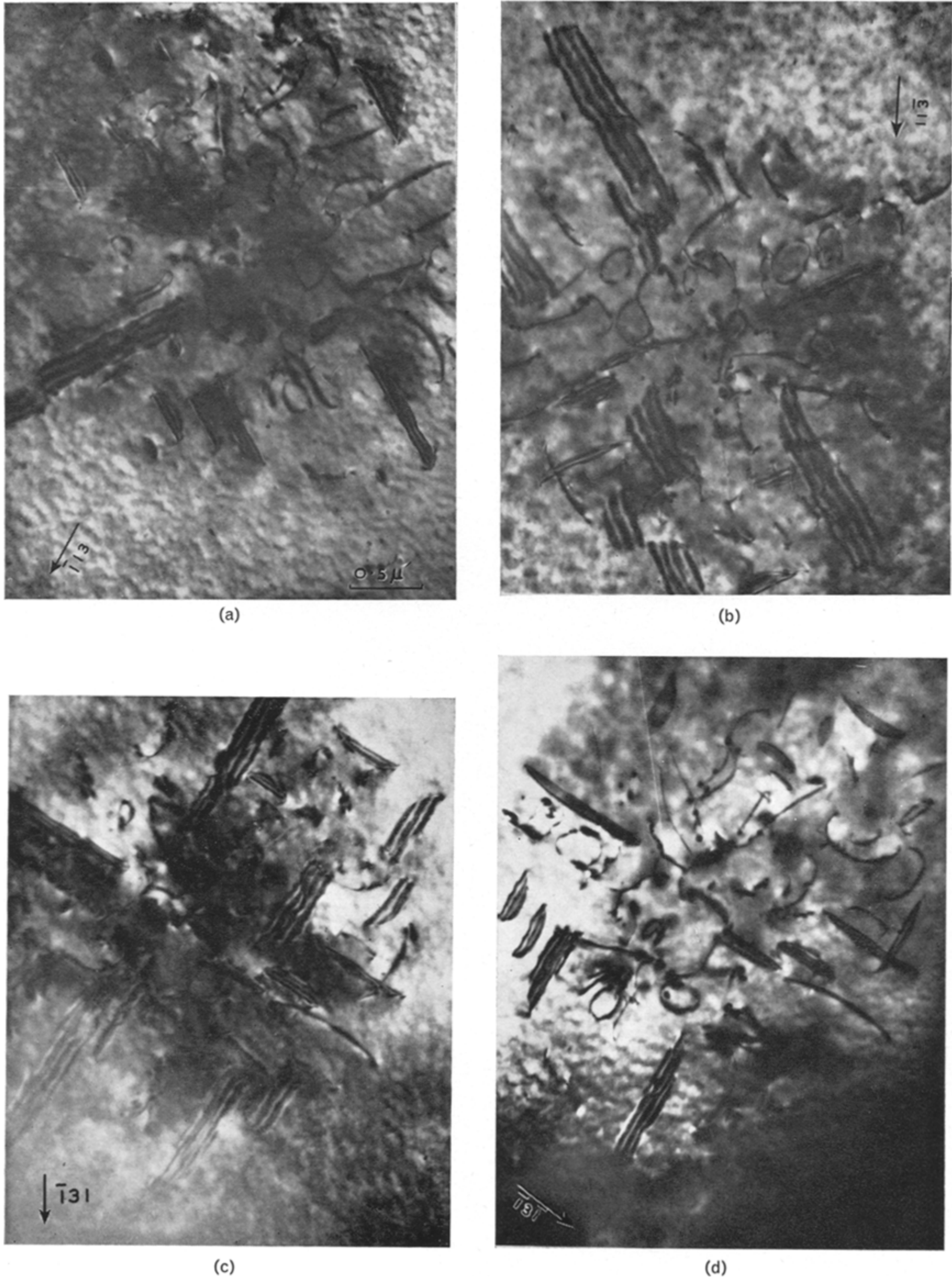

Figure 3 Transmission electron micrographs of stacking-faults showing the images obtained using 311 reflections. (a) $g = \bar{1}13$; (b) $g = 11\bar{3}$; (c) $g = \bar{1}31$; (d) $g = \bar{1}3\bar{1}$ ($\xi_g S_g = 0$). Micrographs (c), (d) have been rotated 58° clockwise with respect to micrographs (a), (b).

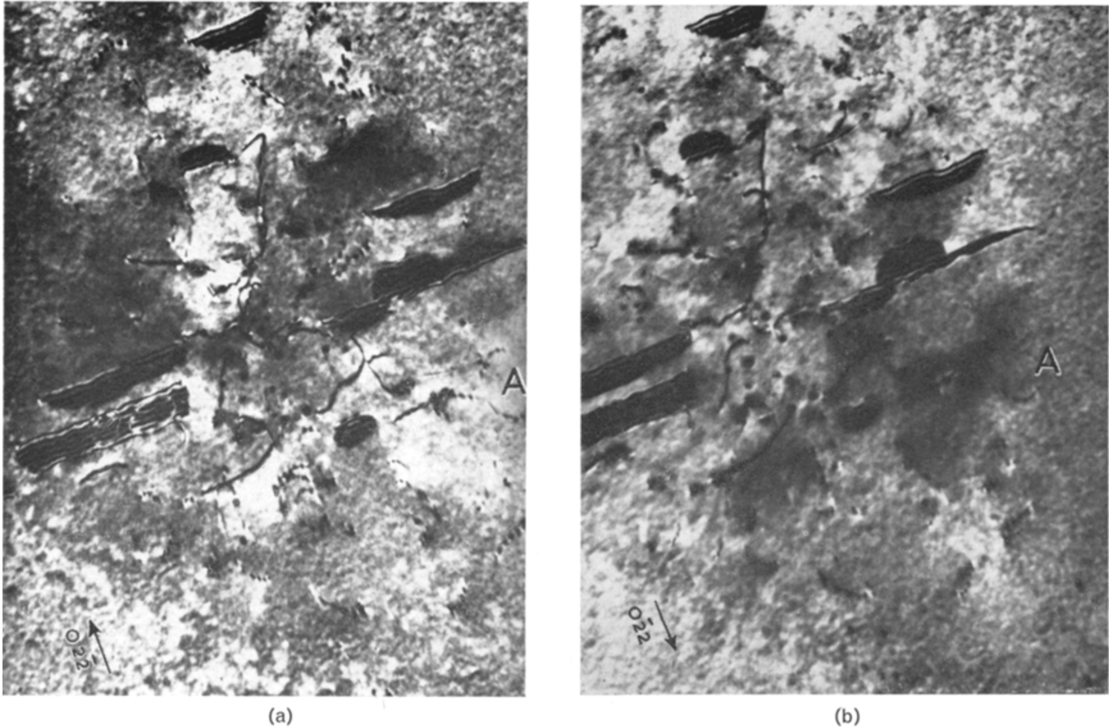

Figure 4 Transmission electron micrographs of stacking-faults showing the effect of reversing the sign of g. (a) $g = 02\bar{2}$; (b) $g = 0\bar{2}2$. The bounding dislocation at A shows strong residual contrast ($\xi_g S_g = 0$).

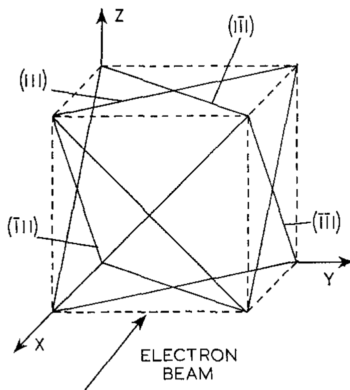

Figure 5 Planes containing the stacking-faults in relation to the direction of the electron beam.

effects at the dislocations bounding the faults is investigated.

3.3. Nature of the Bounding Dislocations

Little can be said at present about the contrast effects arising from the bounding partial dislocations except in the case of single-layer faults and the first layer of multi-layer loops. Here a qualitative analysis can be made by comparing the contrast data with that obtained by Booker and Tunstall [7] in the case of extrinsic faults in silicon. For 220 reflections, when fringe contrast is absent, the bounding dislocation shows oscillatory contrast with the splitting of the contrast at the top surface of the foil, where the image is most intense. This splitting of contrast at the top surface changes from one side of the loop to the other when g is changed (compare the residual contrast at A in figs. 4a, b). The residual contrast is presumably due to the $g \cdot b \wedge u$ product. Therefore, it is possible that for the bounding partial dislocation of the faults, $b = + \frac{1}{3} < 111 >$. Dislocation contrast showing the unusual features seen by Booker and Tunstall [7] using a 400 reflection is also observed for the faults in GaAs (see figs. 2a, b). It is interesting to note that the inner partials bounding the second and third layers show similar contrast effects to that of the outer partials for the same reflection (see figs. 3a, b). Analysis of the bounding partials of the second and third loops is not possible from the data presented here without comparing the observed contrast effects with computed intensity profiles.

Work is in hand to compute profiles in bright field cases using the two-beam dynamical approximation.

4. Discussion

It has been shown that the stacking-faults that are seen in Te-doped GaAs lie on { 1 1 1 } planes and have a fault vector $R = +\frac{1}{3} < 111 >$. This implies the insertion of an extra layer or layers of atoms between the existing layers of the GaAs matrix, resulting in the observed displacement. Meieran [1] suggested that these and associated faults may arise due to some oxide of gallium or arsenic precipitating in the matrix. Abrahams *et al* [3] have suggested that in Se-doped GaAs, precipitates of Ga_2Se_3 occur to a limited extent on {1 1 1} planes and to a larger extent on { 1 1 0 }, {1 0 0} planes and that precipitation is noticeably increased when $N = 10^{18}/cm^3$. In our investigation we observed that the occurrence of stacking-faults increased very rapidly as N became greater than $10^{18}/cm^3$ for both gradient freeze and Czochralski crystals. If the stacking-faults were due to some oxide of Ga or As, the occurrence of the fault regions would be linear along the whole length of the crystal. This is not the case, and so these stacking-faults must be associated with high Te concentration. The stacking-faults could be formed by the aggregation of tellurium by substitution for arsenic in one close-packed layer. Tellurium has a covalent radius of 1.35 Å as compared with 1.19 Å for arsenic. Substitution for arsenic by tellurium would therefore produce an expansion perpendicular to the gallium/tellurium layer and result in an extrinsic fault as is observed. The initiation of the stacking-faults could take place as the temperature during growth is lowered in regions containing a high Te concentration. The formation of the second and subsequent layers will take place when the first layer reaches a critical size. The region containing the faults is one of high strain and is associated with the presence of dislocations. The dislocations can act as channels of easy diffusion to feed the stacking-faults and hence the faults will continue to grow. The precise mechanism by which these faults initially form is not known but the analysis suggests that it could be via the mechanism which Silcock and Tunstall [9] proposed for NbC precipitation in austenitic stainless steels.

In closing, it is interesting to note that Te-doped GaAs exhibits rings of high intensity cathodoluminescence surrounding areas of the same size as the faulted region described here (cf [10, 11].) It is reasonable to suppose that there is an optimum concentration for cathodoluminescence and so these rings probably represent depleted zones surrounding the capture area of stacking-faults.

Acknowledgements

The authors thank the Services Electronics Research Laboratories who supplied the material and much valuable assistance, and Dr G. R. Booker of Oxford University for valuable discussions. We are grateful to Dr M. S. Abrahams for allowing us to see the paper by C. J. Buiocchi [4] prior to publication.

One of us (D.L.) is in receipt of a scholarship from the Science Research Council.

References

1. E. S. MEIERAN, *J. Appl. Phys.* **36** (1965) 2544.
2. M. S. ABRAHAMS and C. J. BUIOCCHI, *J. Phys. Chem. Solids* **28** (1967) 927.
3. M. S. ABRAHAMS, C. J. BUIOCCHI, and J. J. TIETJEN, *J. Appl. Phys.* **38** (1967) 760.
4. C. J. BUIOCCHI, *ibid* **38** (1967) 1960.
5. J. W. EDINGTON and D. R. WEST, *Phil. Mag.* **14** (1966) 603.
6. W. J. TUNSTALL and P. J. GOODHEW, *ibid* **10** (1964) 361.
7. G. R. BOOKER and W. J. TUNSTALL, *ibid* **13** (1966) 71.
8. R. GEVERS, A. ART, and S. AMELINCKX, *Phys. Status Solidi.* **3** (1963) 1563.
9. J. M. SILCOCK and W. J. TUNSTALL, *Phil. Mag.* **10** (1964) 361.
10. D. B. WITTRY and D. F. KYSER, *J. Appl. Phys.* **35** (1964) 2439.
11. D. B. WITTRY, *Appl. Phys. Lett.* **8** (1966) 142.